Quaternary Research 84 (2015) 133–143

Contents lists available at ScienceDirect

Quaternary Research

journal homepage: www.elsevier.com/locate/yqres

Assessing the paleoenvironmental potential of Pliocene to Holocene tufa deposits along the Ghaap Plateau escarpment (South Africa) using stable isotopes

Taylor Louise Doran [a,b,*], Andy I.R. Herries [c,d], Philip J. Hopley [a,b], Hank Sombroek [a], John Hellstrom [e], Ed Hodge [f], Brian F. Kuhn [g]

[a] Department of Earth and Planetary Sciences, Birkbeck, University of London, London WC1E 7HX, UK
[b] Department of Earth Sciences, University College London, London WC1E 6BT, UK
[c] The Australian Archaeomagnetism Laboratory, Department of Archaeology and History, La Trobe University, Melbourne Campus, Bundoora, Vic 3086, Australia
[d] Centre for Anthropological Research, University of Johannesburg, Gauteng, South Africa
[e] School of Earth Sciences, University of Melbourne, Victoria 3010, Australia
[f] Formerly Institute of Environmental Research, ANSTO, PMB1 Menai, NSW 2234, Australia
[g] Evolutionary Studies Institute, University of the Witwatersrand, Johannesburg 2050, South Africa

ARTICLE INFO

Article history:
Received 11 August 2014
Available online 29 May 2015

Keywords:
Tufa
Stable isotope analysis
Radiocarbon dating
Uranium-series dating
Taung
Paleomagnetism

ABSTRACT

The tufa deposits of the Ghaap Plateau escarpment provide a rich, yet minimally explored, geological archive of climate and environmental history coincident with hominin evolution in South Africa. This study examines the sedimentary and geochemical records of ancient and modern tufas from Buxton-Norlim Limeworks, Groot Kloof, and Gorrokop, to assess the potential of these sediments for providing reliable chronologies of high-resolution, paleoenvironmental information. Chronometric dating demonstrates that tufa formation has occurred from at least the terminal Pliocene through to the modern day. The stable isotope records show a trend toward higher, more variable $\delta^{18}O$ and $\delta^{13}C$ values with decreasing age from the end of the Pliocene onwards. The long-term increase in $\delta^{18}O$ values corresponds to increasingly arid conditions, while increasing $\delta^{13}C$ values reflect the changing proportion of C_3/C_4 vegetation in the local environment. Analysis of the Thabaseek Tufa, in particular, provides valuable evidence for reconstructing the depositional and chronological context of the enigmatic Taung Child (*Australopithecus africanus*). Collectively, the results of the present study demonstrate the potential of these deposits for developing high-precision records of climate change and, ultimately, for understanding the causal processes relating climate and hominin evolution.

Introduction

At the south-eastern margin of the Kalahari Desert in the North West Province of South Africa, the dolomitic Ghaap Plateau forms a prominent east–west trending escarpment at the boundary with the quartzites and slates of the Precambrian Transvaal Supergroup (Altermann and Wotherspoon, 1995) (Fig. 1a). The 275 km long escarpment possesses 70–120 m high cliffs from which springs have emerged during the Cainozoic; groundwater exiting the dolomite via these karst springs has deposited layers of tufaceous carbonates that have accumulated as extensive formations over the underlying bedrock and surface deposits (Butzer et al., 1978), which often contain fossils (Peabody, 1954; Curnoe et al., 2005).

In addition to the type specimen of *Australopithecus africanus* (Dart, 1925), an array of vertebrate, fossil material has been recovered from deposits associated with the Ghaap Plateau escarpment tufa formations. These fossiliferous deposits occur in many forms ranging from breccia infillings of small gullies incised into larger formations by karst depositing waterfalls; river-carved rockshelters along the valley walls; vadose caves formed entirely within the tufa; and tufaecous cappings of synchronous forming land surfaces (Humphreys and Thackeray, 1983; Klein et al., 1991; Curnoe et al., 2006; Hopley et al., 2013). Similar to the freshwater carbonate sequences recently described from early hominin localities in the East African Rift Valley (e.g. Johnson et al., 2009; Ashley et al., 2010), the terrestrial carbonates of the Ghaap Plateau escarpment are associated with a long, rich history of hominin occupation in southern Africa from at least the late Pliocene onwards (Humphreys and Thackeray, 1983; Beaumont and Morris, 1990; Beaumont and Vogel, 2006; Hopley et al., 2013).

Not only do the Ghaap tufa deposits preserve a wealth of paleoanthropological and paleolithic materials, these calcareous sediments provide contextual evidence by recording details of landscape evolution. Tufas are terrestrial carbonates formed in freshwater environments

* Corresponding author: 5323 Dover Street, Oakland, CA 94609, USA.
E-mail address: Taylorlouisedoran@gmail.com (T.L. Doran).

http://dx.doi.org/10.1016/j.yqres.2015.04.008
0033-5894/

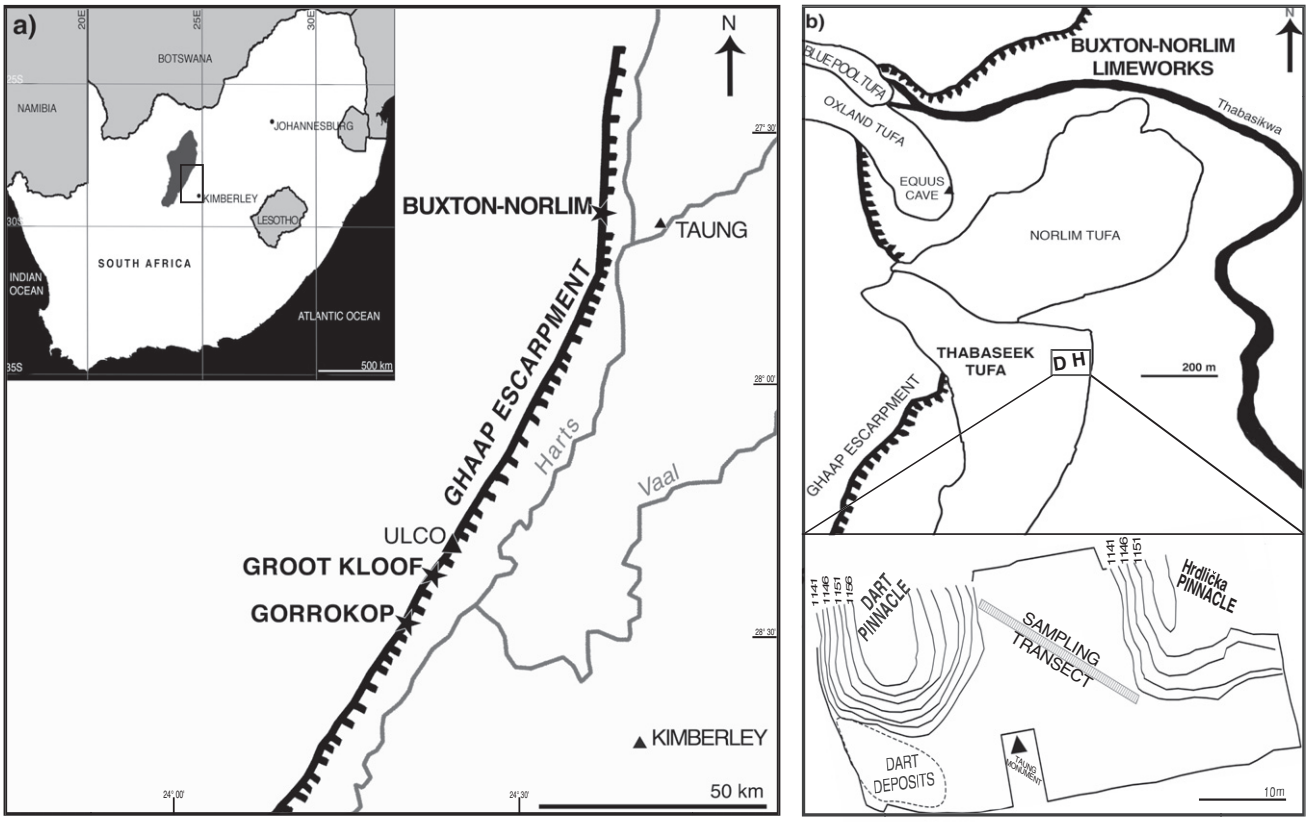

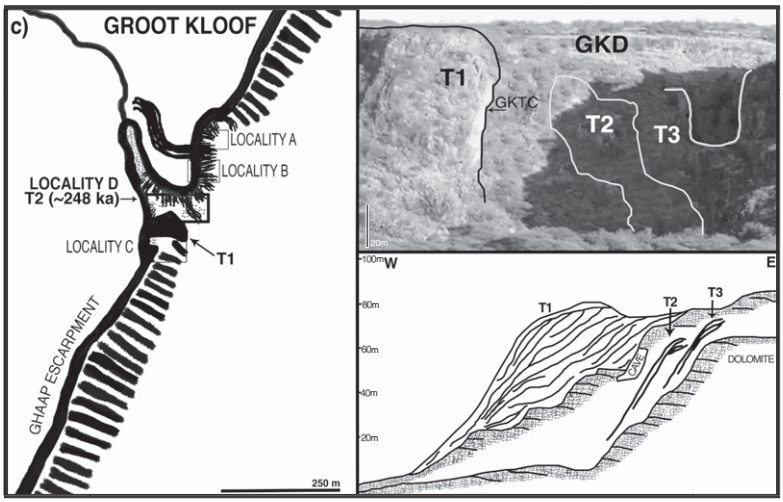

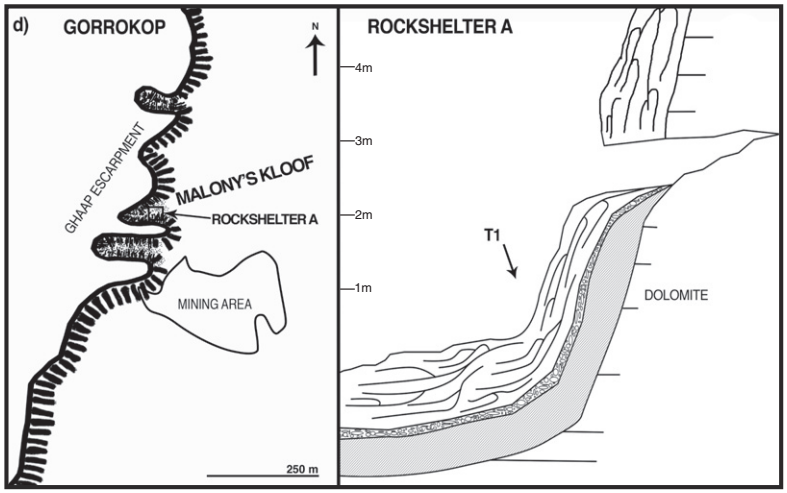

https://doi.org/10.1016/j.yqres.2015.04.008 Published online by Cambridge University Press

under the influence of ambient temperature, alkaline-groundwater discharge through a combination of physiochemical and biologically mediated processes (Pedley, 1990; Ford and Pedley, 1996). Particularly in the semi-arid environment of the Ghaap Plateau, the occurrence of large tufa accumulations is indicative of past humid phases when accelerated groundwater recharge sufficiently enhanced spring flow to permit carbonate formation (Pedley, 1990). As such, tufa deposits comprise important geologic records of past pluvial phases (Nicoll et al., 1999; Viles et al., 2007; Arenas et al., 2014) and may serve as proxy records of hydrological regimes to complement other local proxy records of paleoclimate (e.g., Garnett et al., 2004; Cremaschi et al., 2010; Domínguez-Villar et al., 2011). Previous research on the tufa formations at the sites of Buxton-Norlim, Gorrokop, and Groot Kloof along Ghaap escarpment (Fig. 1a) identified six major geomorphological phases interpreted as representing changing climatic conditions (Butzer, 1974; Butzer et al., 1978). While this initial research provided the first long-term record of moisture and temperature changes in the region (Butzer et al., 1978), the capacity of the Ghaap tufa deposits to further provide high-resolution information about the climatic factors controlling hydrological processes through geochemical and geochronological analyses remains largely unexplored.

To assess the chronometric and paleoenvironmental value of the Ghaap Plateau escarpment tufas, we examined modern and ancient deposits from three localities, the Buxton-Norlim Limeworks near Taung, and Groot Kloof and Gorrokop, containing Malony's Kloof, near Ulco (Fig. 1a). Tufa deposits were dated using radiocarbon, uranium–thorium, and paleomagnetic methods, while sedimentary and stable isotope records were analysed as paleoenvironmental proxies. The collective results from our analyses highlight the value of these terrestrial carbonates as chronologically reliable archives of paleoenvironmental conditions (Pentecost, 2005; Andrews, 2006), particularly in this semi-arid region central to the study of human evolution.

Materials and methods

The massive tufa fan deposits spanning the length of the Ghaap Plateau escarpment are particularly well-developed in the areas of Taung (Buxton-Norlim Limeworks) and Ulco (Groot Kloof and Gorrokop) (Fig. 1a). At Buxton-Norlim, on the north-eastern edge of the escarpment, discharge from the groundwater fed Thabaseek River has deposited extensive tufa formations since the Pliocene (Fig. 1b; Peabody, 1954; Butzer, 1974; McKee, 1993a,b). In 1924, lime quarry operations along the eastern edge of the southernmost Thabaseek Tufa formation yielded the Taung Child skull, which provided the first fossil evidence for an ape-like human ancestor and the type specimen of *A. africanus* (Dart, 1925). Continued mining operations destroyed the provenance of the skull and much of the geological context, however, two pinnacles, known as the Dart and Hrdlička pinnacles, were left in place on either side, and slightly north, of the suspected discovery site (Partridge, 2000). Recent investigations demonstrate that the Taung Child skull derives from a calcrete horizon overlain and underlain by the Thabaseek Tufa (Hopley et al., 2013). Additionally, remnants of at least 17 Pleistocene and Holocene fossil sites have also been identified within the tufa deposits at Taung (McKee, 1994).

About 100 km southwest along the escarpment, in the area of Ulco, a series of large tufa fans and carapaces have been deposited along drainage lines related to the Steenkop River (Fig. 1a; Butzer et al., 1978). The oldest deposits at these karstic complexes have been eroded through by streams to form a series of caves, rock shelters, and canyons (Kloofs) containing lithic- and fossil-bearing deposits, which are concentrated at two main locations, Groot Kloof and Malony's Kloof (Butzer, 1974; Butzer et al., 1978; Beaumont and Vogel, 1993; Curnoe et al., 2005, 2006; Herries et al., 2007). At the larger site of Groot Kloof ('Great Ravine'), locality GKD is the main gorge comprising the most extensive, ancient formation (T1), as well as a steeply dipping waterfall tufa (T2) (Fig. 1c). The lower GKD deposits contain Earlier Stone Age tools that have been preliminarily ESR dated to ~1.0–0.8 Ma (Blackwell et al., 2012). Additionally, T2 contains *in situ* stone tools that have not been attributed to a specific industry, but have been uranium-series dated to Marine Oxygen Isotope Stage (MIS) 7 (248 ± 37 ka; Curnoe et al., 2006), coeval with the formation of the Oxland Tufa at Taung (256 ± 21 ka: Vogel and Partridge, 1984), and suggesting contemporaneous formation of the deposits at both sites (Butzer et al., 1978). Slightly further south again is the active tufa complex of Gorrokop mined in the late 1980s. A section, known as Malony's Kloof, consists of remnant tufa deposits into which a series of rockshelters have been eroded as part of the development of the kloof (Fig. 1d). At Malony's Kloof Rock Shelter A (MKA), a calcified 8 m long talus slope is reinforced by tufa deposits that have subsequently been weathered by drip water and later infilled with soft sediments. Breccia deposits from the opening of MKA contain microlithic stone tools characteristic of an early Later Stone Age style assemblage and Florisian fauna (Herries et al., 2007).

A small number of hand specimens were collected from the Plio-Pleistocene Thabaseek Tufa between the Dart and Hrdlička Pinnacles at Buxton-Norlim (Fig. 1b), as well as from tufa formations of various ages at Groot Kloof (Fig. 1c) and Gorrokop, including Malony's Kloof (Fig. 1d) for chronometric and paleoenvironmental analyses. The field characteristics and localities of eleven hand specimens selected for petrographic and geochemical analyses are listed in Table 1. To investigate the calcite fabric and microstructure, thin sections were made and viewed under a polarizing microscope; some selected samples were also subjected to quantitative mineralogical analysis by X-ray diffraction (XRD). Stable isotope subsampling was carried out on polished, cut sections from each of the eleven hand specimens. Detailed descriptions of the analytical procedures are provided in the Supplementary data.

Results

Dating results

Measured AMS $^{14}C/^{13}C$ ratios were converted to conventional radiocarbon ages after background subtraction and ^{13}C fractional correction (437 ± 103 yr) (Supplementary data), and were calibrated using OXCAL 4.2 and the ShCal13 curve (Hogg et al., 2013).

A comparison of a dead carbon fraction (DCF) corrected C^{14} age and U–Th age for the same samples gave consistent ages (Tables 2 and 3). Tufa sample GKD_C14_05 was dated to 5.4 ± 0.2 cal ka BP by AMS ^{14}C and 5.8 ± 5.2 ka by U–Th, demonstrating close alignment. Likewise, sample MKA_06_C14_04 was dated to 10.7 ± 0.2 cal ka BP by AMS ^{14}C and 11.6 ± 6.2 ka by U–Th, also showing good correspondence. DCF changes have only a small relative effect on the final age of 'old' tufa samples and AMS ^{14}C offers good age control for the tufas in the time range of 44–0 cal ka BP. Significant detrital Th contributed to the large 1σ uncertainty associated with these ages and accounts for a larger overlap with both ^{14}C ages, yet the average U–Th ages calculated are still very similar. Both ^{14}C ages are slightly younger than their U–Th

Figure 1. a) Locations of Buxton-Norlim, Groot Kloof, and Gorrokop (containing Malony's Kloof) along the Ghaap Plateau (after Butzer, 1974). Inset shows the position of the Ghaap Plateau (shaded) within South Africa. b) Overview of the formations at the Buxton-Norlim Limeworks as reconstructed by Peabody (1954) showing the Thabaseek Tufa with the outcrop localities of the Dart Pinnacle (D) and Hrdlička Pinnacle (H) (above); diagram of the remnant Dart and Hrdlička pinnacles (27°37′10″S, 24°37′ 59″E) and the NW–SE sample collection transect (dashed line) (below) (after McKee, 1993b). c) Diagram of Groot Kloof (28°34′ 89″S, 24°18′ 23″E) within the escarpment of the Ghaap Plateau (after Butzer, 1974) (left); view of Groot Kloof Locality D (GKD) showing the major site features — Tufa 1 (T1), Tufa 2 (T2), Tufa 3 (T3), the Groot Kloof Tufa Cave (GKTC) (after Curnoe et al., 2006) (above right); generalized cross-section of the GKD tufa formations (after Butzer, 1974) (below right). d) Diagram of the localities of Gorrokop and Malony's Kloof (28°36′98″S, 24°16′69″E) within the escarpment of the Ghaap Plateau (left); generalized cross-section of Malony's Kloof Rockshelter A with tufa sample locations (right).

https://doi.org/10.1016/j.yqres.2015.04.008 Published online by Cambridge University Press

Table 1
Field characteristics, internal fabrics and crystallography, and mineralogical composition of Ghaap Plateau Escarpment tufa deposits used in the paleoenvironmental study.

Sample name	Locality	Lithology	Colour	Morphology	Mineralogy	Date
TDPC 2	Taung, Thabaseek Tufa	Thrombolic tufa	White	Thrombolitic phytoherm tufa with fenestral porosity lined with clear, isopachous dogtooth spar. Turbid, biomediated microspar is associated with clotted peloids.	Calcite	Plio-Pleistocene
TDPC 7	Taung, Thabaseek Tufa	Thrombolic tufa	White	Thrombolitic phytoherm tufa with cyanobacterial filaments and calcite spar. Porosity is arranged in branching networks that represent the casts of hydrophytic plant stems. Cross-sections through higher plant leaves show remnant leaf structure.	Calcite	Plio-Pleistocene
TDPC 16	Taung, Thabaseek Tufa	Thrombolic tufa	White	Thrombolitic phytoherm tufa with fenestral porosity and *Vaucheria* filaments. Tufa is partly laminated with undulose horizons comprising alternations of micrite and spar, interspersed with quartz-rich detrital laminae, possibly representing flooding events. Ostracodes present. Dedolomitised relicts of zoned dolomite.	Calcite, dedolomite/ dolomite	Plio-Pleistocene
TDPC 26	Taung, Thabaseek Tufa	Thrombolic tufa	White	Thrombolitic phytoherm tufa superimposed on a framework of hydrophyte stem casts which form a fenestral porosity. An isopachous radiaxial fibrous calcite cement encrusts the outside and inside of macrophyte stems and dolomite and dedolomite fills some macrophyte stem moulds.	Calcite, dedolomite/ dolomite	Plio-Pleistocene
MKPM1	Ulco, Malony's Kloof main tufa	Stromatolitic tufa	White to brown	Stromatolitic, crenulated laminae with abundant microbial and algal inclusions; almost complete secondary cementation of void space; silt-sized quartz grain inclusions.	Calcite, quartz	Plio-Pleistocene
MKA_03	Ulco, Malony's Kloof main tufa	Stromatolitic tufa	Light pink to dark brown	From base, dense, crenulated laminae of organic and calcite bands with monocrystalline quartz inclusions; high degree of secondary cementation of fenestral voids increasing in primary and secondary porosity towards top.	Calcite, quartz	Plio-Pleistocene
GKD_UTH_01	Ulco, Groot Kloof T2 flow	Stromatolitic tufa	White to dark brown	Planar to wavy laminae of mud-rich and sparry calcite bands; numerous microbial inclusions; increasing porosity and organic inclusions (fenestral voids) towards top of thin section.	Calcite, quartz	Middle Pleistocene
GKDPM2	Ulco, Groot Kloof T2 flow	Stromatolitic tufa	Light pink to dark brown	Dense, alternating stromatolitic layers of light spar calcite and dark micrite laminae; primary equant spar calcite, peloidal micrite; fenestral voids commonly filled with secondary columnar cement; sub-angular, size sorted detrital quartz inclusions throughout.	Calcite, quartz	Middle Pleistocene
GKD_UTH_08	Ulco, Groot Kloof, W2 flow	Bryophyte tufa	Dull gray	Highest primary porosity displaying almost complete lack of cementation with minimal isopachous rim cement; very fine-grained cryptocrystalline calcite.	Calcite, aragonite, quartz	Upper Pleistocene
GKD_UTH_04	Ulco, Groot Kloof, tufa on dolomite	Stromatolitic tufa	Light pink to light brown	Crenulated alternating dark and light laminae with abundant fenestral voids increasing towards top of specimen; some secondary infilling by micritic cement; homogenous, monocrystalline quartz grains dispersed throughout, not confined to a particular layer.	Calcite, quartz	Holocene
GKD_C14_04	Ulco, Groot Kloof, tufa on dolomite	Stromatolitic tufa	Light to dark brown	From base planar alternating laminae and fenestral voids; increasingly porous towards top; spongy micrite cement.	Calcite, quartz	Holocene

counterparts, which may indicate that the DCF correction has been over-estimated. However, at 5.3 ± 1.2%, it is already significantly lower than that applied in other studies (e.g. Horvatinčić et al., 2003) and the uncertainties of the U–Th ages do not allow for a more accurate appraisal.

Micromorphology results

The main micromorphological characteristics and primary mineral components of eleven hand specimens analysed as paleoenvironmental proxies are listed in Table 1. The Thabaseek Tufa specimens studied (TDPC 2, 7, 16, 26) can all be classified as phytoherm boundstones (Pedley, 1990) or as microphytic thrombolitic tufa (Carthew et al., 2006). The microfacies is characterised by a three-dimensional thrombolitic texture in which microbial carbonate outlines form irregular equidimensional clots – formed of smaller clots internally. In thin section, the Thabaseek Tufa specimens consist of micrite, peloids, fenestral pores, and phytomoulds of calcite-encrusted hydrophytic plant stems (Fig. 2a). All Thabaseek thin sections contain a fenestral porosity

Table 2
Radiocarbon ages for tufa samples from Groot Kloof and Malony's Kloof.

Sample name	Sample locality	^{14}C age (^{14}C yr BP)	1 sigma error (^{14}C yr)	DCF corrected ^{14}C age (^{14}C yr BP)*	1 sigma error (^{14}C yr)	Calibrated age (cal yr BP)#	1 sigma error (cal yr)
GKD_C14_04	GK T4	779	41	342	144	**268**	**134**
GKD_UTH_04	GK T4	2577	64	2140	167	**2097**	**199**
MKA_06_C14_02	MKA capping	4510	60	4073	163	**4484**	**204**
GKD_C14_05	GK T4	5179	61	4742	164	**5354**	**198**
MKA_06_C14_04	MKA capping	9900	85	9463	188	**10,717**	**234**
GKD07_UTH_07	GK T3	35,814	676	35,377	779	**40,031**	**773**
GKD_UTH_02	GK T3	40,771	823	40,334	926	**44,132**	**766**
GKD_UTH_08	GK T3	40,993	796	40,556	899	**44,270**	**757**
MKA_03	MK main tufa	54,304	4032	53,867	4135	**Infinite**	**Infinite**

The columns in bold, calibrated ages and 1 sigma error, contain ages quoted in the text.
* DCF correction = 5.3 ± 1.2%, equivalent to a 437 ± 103 yr offset.
\# Calibrated using the OXCAL 4.1 calibration software and the ShCal13 data sets (Hogg et al., 2013).

https://doi.org/10.1016/j.yqres.2015.04.008 Published online by Cambridge University Press

Table 3
Uranium–Thorium dates for samples from Groot Kloof and Malony's Kloof.

Sample name	Tufa phase	U^{238} ng/g	$^{230}Th/^{238}U$ (a)	$^{232}Th/^{238}U$ (b)	$^{232}Th/^{238}U$	$^{230}Th/^{232}Th$	$^{234}U/^{238}U$ (c)	Age (ka) (d)	2*se*
GKD_UTH_13	T1	309	2.0816 (0.0058)	1.8452 (0.0034)	0.187801 (0.001940)	3.4751 (0.0427)	11.1	**369.4**	12.3
MKA_C1_01	T2	19	1.2586 (0.0163)	1.2718 (0.0177)	0.116885 (0.004062)	1.6138 (0.0282)	10.8	**275.4**	29.4
GKD_UTH_12	T2	91	1.6537 (0.0129)	1.7089 (0.0050)	0.051171 (0.000948)	2.3415 (0.0185)	32.3	**221.4**	6.3
GKD_UTH_11	T2	66	1.3619 (0.0203)	1.8288 (0.0077)	0.013163 (0.000339)	2.1927 (0.0148)	103.5	**127.4**	3.5
MKA_04	T4	114	0.3072 (0.0046)	2.0341 (0.0090)	0.072686 (0.001032)	2.0869 (0.0094)	4.2	**11.6**	6.2
GKD_C14_05	T4	131	0.2149 (0.0032)	2.2566 (0.0071)	0.067679 (0.000892)	2.2956 (0.0074)	3.2	**5.8**	5.2

a) Numbers in brackets are 95% uncertainties of the given least significant figures; b) activity ratios determined after Hellstrom (2003) using the decay constants of Cheng et al. (2000). Numbers in brackets are 95% uncertainties of the given least significant figures; c) initial ($^{234}U/^{238}U$) calculated using corrected age; and d) bold ages in ka before present corrected for initial ^{230}Th using eq. of Hellstrom (2006) quoted in text.

that is often associated with branching, bifurcating networks of subvertical casts of hydrophytic plant stems (2–4 mm in cross-section of hand specimens). In TDPC 7, the thrombolite is characterised by a grumose texture of clotted peloids, which is superimposed upon a framework of inclined algal filaments and *in situ* hydrophytic plant stems, the subaqueous parts of which became encrusted by radial calcite spar cement during growth (Fig. 2b). The prevalence of hydrophilic plants in the form of these mouldic pores filled by alternating envelopes of spar and micrite suggests that these deposits formed subaqueously, in the vicinity of a palustrine environment, in a position peripheral to a flowing channel or on the margins of the slow-flowing and pooled areas where hydrophilic vegetation would have grown thickly and protected encrusting biofilms (Vàzquez-Urbez et al., 2012). The low detrital component (<1% of thin section), dearth of phytoclastic intervals, absence of bryophytes and oncoids (with one possible exception), and widespread occurrence of ostracodes, suggests these are phytoherm tufas that formed in a subaqueous, dominantly sluggish water pool environment, probably at the margins of ponded areas behind barriers (see Supplementary data for full results) (Arenas et al., 2007).

The Groot Kloof and Malony's Kloof tufas are a combination of phytoherm framestone and phytoherm boundstone deposits (Pedley, 1990), characterised largely by stromatolitic facies. In thin section, the laminar structure is generally constituted by alternated millimetric light sparitic to dark micritic calcite laminae ranging from planar to wavy and distinguished by differences in colour, thickness, and crystal formations, with variations in porosity and microbial inclusions (Jones and Renaut, 2010). The decay of organic inclusions has also generated void space, which has either remained empty or secondarily in-filled by micrite, isopachous rim cement, sparry calcite, and drusy mosaic cements. While all of the thin sections of the Ulco tufas are cemented

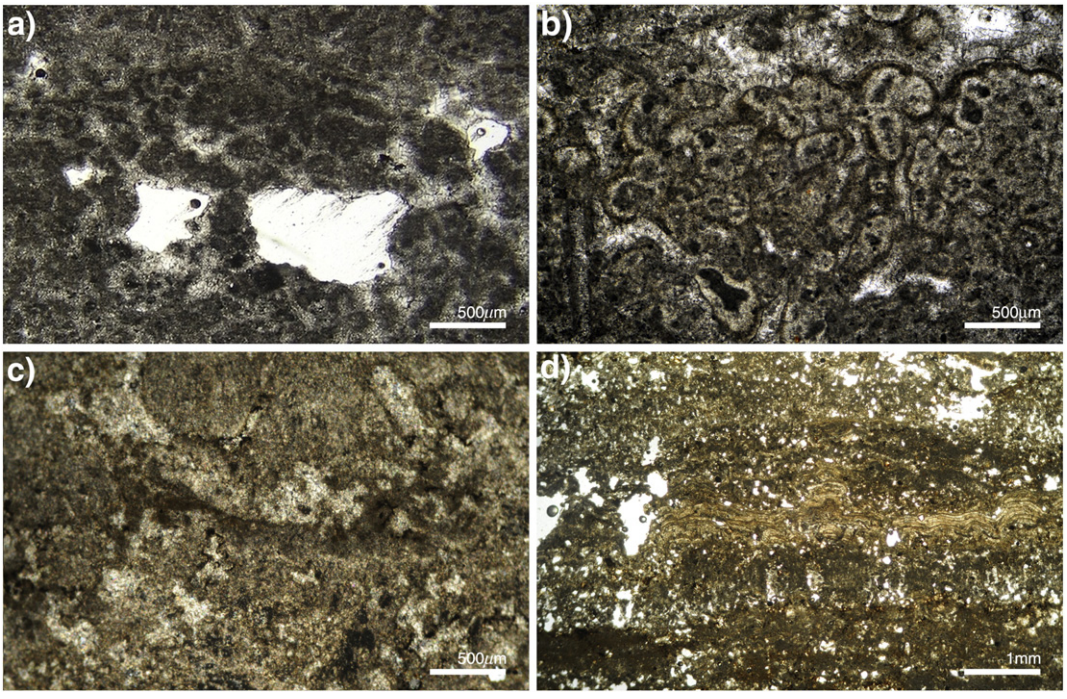

Figure 2. Micrographs of the Thabaseek Tufa and Groot Kloof tufa thin sections (under crossed polarised light). a) Thrombolitic texture of the Thabaseek Tufa showing micrite, peloids, fenestral porosity (TDPC 2; ppl width of view 4.5 mm). b) Linear filamentous fabric seen in transverse to oblique view of a phytoherm boundstone of microstems (algal filaments) encrusted by isopachous radial calcite spar (TDPC 7; ppl width of view 2.2 mm). c) Calcitization and cementation of void space characterising the ancient Ulco specimens (lower part of GKD_UTH_01; ppl width of view 3 mm). d) Dense planar to wavy laminae showing primary porosity of younger Groot Kloof deposits (GKD_UTH_04; ppl width of view 7 mm).

https://doi.org/10.1016/j.yqres.2015.04.008 Published online by Cambridge University Press

Table 4
The mean, maximum, and minimum $\delta^{18}O$ and $\delta^{13}C$ values for the Ghaap Plateau escarpment tufa.

Sample site	Sample name	$\delta^{18}O$			$\delta^{13}C$			Number of analyses
		Mean	Min	Max	Mean	Min	Max	
Buxton-Norlim, Thabaseek Tufa	**TDPC 2**	−6.4‰	−6.5‰	−6.1‰	−6.7‰	−6.7‰	−6.5‰	3
	TDPC 7	−5.9‰	−6.0‰	−5.8‰	−6.8‰	−7.0‰	−6.7‰	3
	TDPC 16	−5.8‰	−5.9‰	−5.7‰	−5.6‰	−5.9‰	−5.4‰	3
	TDPC 26	−5.9‰	−6.0‰	−5.9‰	−6.7‰	−6.8‰	−6.6‰	3
Ulco, Malony's Kloof	**MKPM1**	−5.2‰	−5.3‰	−5.1‰	−7.6‰	−7.6‰	−7.5‰	3
	MKA_03	−5.3‰	−5.5‰	−4.9‰	−7.7‰	−7.8‰	−7.3‰	8
		(−4.9‰)		(−1.9‰)	(−6.6‰)		(1.9‰)	(9)
Ulco, Groot Kloof	**GKD_UTH_01**	−3.3‰	−3.8‰	−2.5‰	−3.4‰	−3.7‰	−2.9‰	6
		(−3.1‰)		(−2.0‰)	(−3.1‰)		(−1.5‰)	(7)
	GKDPM2	−3.8‰	−4.7‰	−3.5‰	−3.8‰	−5.1‰	−3.0‰	17
	GKD_UTH_08	−3.0‰	−3.4‰	−1.9‰	−1.4‰	−1.9‰	−0.5‰	6
	GKD_UTH_04	−2.1‰	−2.6‰	−1.3‰	−0.9‰	0.3‰	1.2‰	6
	GKD_C14_04	−1.9‰	−2.9‰	−0.4‰	−0.7‰	−0.4‰	1.4‰	5

() The bracketed statistics in MKA_03 and GKD_UTH_01 are inclusive of the divergent values of the respective uppermost sampling on both specimens (MKA_03_Sample01; GKD_UTH_01_Sample01), which are interpreted as representing more recent growth.

to some degree, those sampling ancient formations at Groot Kloof and Malony's Kloof (GKD_UTH_01, GKDPM2, MKPM1, MKA_03) (Fig. 2c) exhibit more complete cementation relative to those from modern deposits (GKD_UTH_04, GKD_C14_04) (Fig. 2d). It is notable, however, that the upper ~1–2 cm strata of MKA_03 and GKD_UTH_01, evince a marked increase in void space and fenestral porosity, which contrasts the high degree of cementation observed in the respective basal sections (Supplementary data). As such, the top layers of both GKD_UTH_01 and MKA_03 deposits are interpreted as recent coatings of calcite deposited upon the respective older formations, which is confirmed by radiocarbon ages for MKA_03 discussed further below.

Stable isotope results

The stable isotope data for the Ghaap Plateau escarpment tufas analysed are summarised in Table 4 (see Supplementary data for full results). The Thabaseek Tufa (TDPC 2, 7, 16, 26) samples yielded relatively light $\delta^{18}O$ and $\delta^{13}C$ values with overall means of −6.0‰ and −6.5‰, respectively. Similarly, the Malony's Kloof T1 (MKPM1, MKA_03) specimens also have consistently light values with the exception of the uppermost sample from the Malony's Kloof Rock Shelter A tufa deposit (MKA_03_Sample01). The anomalously high $\delta^{18}O$ and $\delta^{13}C$ (−1.9‰ and 1.9‰, respectively) of this sample correspond with the micromorphological incongruities observed in the top portion of the deposit. Overall, the clustered values of the Thabaseek Tufa and Malony's Kloof tufa deposits contrast the variation observed amongst the Groot Kloof tufas. The five recent and ancient specimens sampling formations at the latter site display relatively heavier oxygen and carbon isotopes, as well as a higher degree of variability. $\delta^{18}O$ values ranged from −4.7‰ (GDKPM2) to close to zero (−0.4‰ in GKD_C14_04), while $\delta^{13}C$ values ranged from −5.1‰ (GDKPM2) to 1.4‰ (GKD_UTH_04). This range in variation appears to be related to the assorted ages of the samples where the more ancient deposits, GKDPM2 and GKD_UTH_01, generally have lighter stable isotopes versus the heavier, more variable isotopic compositions of the younger deposits (GKD_UTH_08, GKD_UTH_04, GKD_C14_04). Only GKD_UTH_01 diverges from this pattern in a manner similar to MKA_03. The uppermost sample of GKD_UTH_01 (GKD_UTH_01_Sample01), also displays conspicuously heavier stable isotopes ($\delta^{18}O$: −2.0‰, $\delta^{13}C$: −1.5‰) relative to the mean of those sampling the base of the deposit ($\delta^{18}O$: −3.1‰; $\delta^{13}C$: −3.1‰), and, likewise, correspond to the petrographic differences observed in the top of the deposit. Along with the combined results from geochronological analyses, the tufa deposits used in the present study can be grouped into three main temporal periods, the Pliocene, Middle Pleistocene, and Terminal Pleistocene–Holocene, based on stable isotope compositions reflecting deposition under distinct paleoclimatic regimes.

Pliocene (TDPC 2, 7, 16, 26; MKPM1; MKA_03)

The first group, representing the oldest deposits, consists of the Pliocene Thabaseek Tufa and the Malony's Kloof T1 specimens. The Thabaseek Tufas at the Buxton-Norlim Limeworks record a *normal* magnetic polarity, while sediments infilling caves formed within these deposits record a reversed polarity (Hopley et al., 2013). Based on fauna associated with these tufas infills (McKee, 1993a), the *normal* polarity of the Thabaseek tufa exposed between the Dart and Hrdlička Pinnacles (TDPC 2, 7, 16, 26) is likely related to the end of the Pliocene Gauss Chron between 3.03 and 2.58 Ma, whereas the reversed polarity of the cave fills is likely related to the beginning of the early Pleistocene Matuyama Chron between 2.58 and 1.95 Ma (Herries et al., 2013). At Groot Kloof, the canyon formed through the oldest tufa deposit (T1) has been partially in-filled by a number of later tufa deposits that have been U–Th dated to as old as 369 ± 12 ka, which demonstrates not only the amenability of certain parts of tufa deposits to U–Th dating, but also a minimum age for the oldest T1 deposit (Table 3). The T1 tufa also has a *normal* magnetic polarity, and as such, may not be older than the Brunhes–Matuyama boundary at 780 ka, the last major reversal of the Earth's magnetic field. However, Electron Spin Resonance analyses on a lechwe (*Kobus leche*) tooth from calcified sediments at GKD provided an age range of 1.05–0.80 Ma (Blackwell et al., 2012), and thus, the *normal* magnetic polarity may correspond to the Jaramillo Subchron (1.07–0.98 Ma), or could, as Butzer (1974; et al., 1978) hypothesised, be the same age as the *normal* polarity Thabaseek Tufa at Taung.

At Gorrokop, the oldest tufa deposit through which Malony's Kloof has been eroded also records a *normal* magnetic polarity (MKPM1), while the radiocarbon 'infinite' age (MKA_03) indicates that the age of the deposits exceeded the limits of this dating technique (<50 ka) (Table 2). The oldest dated sample at Malony's Kloof comes from the Tufa 2 (T2) deposit that formed within the kloof itself and has yielded age of 275 ± 29 ka (Table 3) thereby showing a similar pattern of formation to Groot Kloof. The oldest well-dated tufas from both Groot Kloof and Malony's Kloof are thus at least Middle Pleistocene in age. Given the weathered nature of stratigraphically older Malony's Kloof T1, however, it is possible that Pliocene tufas exist at both Ulco localities, as at the Buxton-Norlim Limeworks. The stable isotope records from the Malony's Kloof T1 tufa, which groups with those of the Thabaseek Tufa, may confirm a much earlier, similarly Pliocene age, for this formation. Excluding MKA_03_Sample01 that groups with the younger Ghaap tufas from Groot Kloof, the Thabaseek Tufas and Malony's Kloof T1 deposits record the lowest $\delta^{18}O$ values ranging from −6.5‰ to −4.9‰ (mean = −5.8‰), and even more distinctly, the lowest $\delta^{13}C$ values ranging from −7.8‰ to −5.4‰ (mean = −6.0‰) (Table 4). Within this Pliocene group, the Thabaseek tufa deposits have slightly higher

https://doi.org/10.1016/j.yqres.2015.04.008 Published online by Cambridge University Press

$\delta^{13}C$ values compared to those from the MKA T1 formation. The tight clustering of the $\delta^{18}O$ and $\delta^{13}C$ values from the Malony's Kloof deposits, in particular, highlights not only the uniformity of isotope records obtained from the same tufa formation, but also the disparity in climatic conditions associated with the more recent formation of the uppermost strata (MKA_03_Sample01).

Middle Pleistocene (GKDPM2; GKD_UTH_01)

The second group comprises the middle Pleistocene Tufa 2 (T2) deposits from Groot Kloof with ages between 380–124 ka (GKD_UTH_01, GKDPM2). A preliminary U–Th age of 248 ± 37 ka (Curnoe et al., 2006) for a well-laminated, non-porous tufa (GKDPM2) from T2 indicates that the younger tufas at Groot Kloof are as old as the Middle Pleistocene. Further U–Th dating of tufa infillings from T2 suggest deposition occurred during a number of interglacial periods: 369 ± 12 ka (MIS11-10 transition), 221 ± 6 ka (MIS7), and 127 ± 3 ka (MIS 5) (Table 3), including, by association, Groot Kloof specimen GKD_UTH_01, which has not yet been dated. In conjunction with a 275 ± 29 ka (MIS 9) age from Malony's Kloof, these collective ages for the Ghaap tufa cover the last 4 interglacial periods. While GKD_UTH_12 (221 ± 6 ka) formed during MIS7, the ages are such that it may have fallen in the cold substage 7d. On the other hand, any relatively recent uranium mobility within the samples would have had the largest impact on the oldest samples, which might, for instance, actually represent MIS 7a/c, 7d, and 9; the current data set for each sample, however, is too limited to allow for identification of any such trends. These Middle Pleistocene T2 deposits from Groot Kloof (GKD_UTH_01; GKDPM2) show higher and, more variable isotopic compositions (Table 4). Not including the uppermost sample of GKD_UTH_01 (Sample01), which plots within the terminal Pleistocene–Holocene deposits, the $\delta^{18}O$ values in this group range from −4.7‰ to −2.5‰ (mean = −3.7‰), while $\delta^{13}C$ values range from −5.1‰ to −3.0‰ (mean = −3.6‰) (Table 4).

Terminal Pleistocene–Holocene (GKD_UTH_08, GKD_UTH_04, GKD_C14_04)

A series of tufa deposits formed within an eroded canyon of a middle Pleistocene tufa deposit (T3) at Groot Kloof yielded comparable ages of 44 ± 0.8 cal ka BP (GKD_UTH_08), 44 ± 0.8 cal ka BP, and 40 ± 0.8 cal ka BP (Table 2). Tufa samples forming on the dolomite wall of Groot Kloof (GKT4) produced Holocene ages of 5.4 ± 0.2 cal ka BP, 2.1 ± 0.2 cal ka BP (GKD_UTH_04), and the last few 100 yr (0.3 ± 0.1 cal ka BP: GKD_C14_04) (Table 3), while ICPMS U–Th methods yield ages of 5.8 ± 5.2 ka (Table 3). At Malony's Kloof Rock Shelter A (MKA), tufa samples from cemented early Later Stone Age and Florisian (>10 ka) fossil bearing deposits (Curnoe et al., 2006) were dated using ^{14}C methods to 11 ± 0.2 cal ka BP and 4.5 ± 0.2 cal ka BP (Table 2). These are consistent with a potential Holocene age for the outer layers of MKA_03 (Sample01), which record the highest $\delta^{18}O$ and $\delta^{13}C$ values that plot with these younger deposits. Thus, the third group comprises the terminal Pleistocene to Holocene specimens from Groot Kloof (GKD_UTH_08; GKD_UTH_04; GKD_C14_04), as well as the top samples from MKA_03 (Sample01) and GKD_UTH_01 (Sample01), which collectively show the highest isotope values, as well as the highest degree of variability. $\delta^{18}O$ values of this group range from −3.4‰ (GKD_UTH_08) to −0.4‰ (GKD_C14_04), while $\delta^{13}C$ values range from −1.9‰ (GKD_UTH_04) to 1.9‰ (MKA_03) (Table 4). The isotopic variability observed within these deposits is likely a reflection of the fact they include tufas of not only interglacial (late Holocene samples: GKD_UTH_04; GKD_C14_04), but also upper Pleistocene glacial age (GKD_UTH_08: ~44 ka), unlike the older Middle Pleistocene Group deposits (GKDPM2; GKD_UTH_01).

Discussion

Patterns in the timing of tufa growth

The collective dating results of the present study, which are compatible with previously reported ^{14}C ages for Groot Kloof and Gorrokop tufa (Butzer et al., 1978; Beaumont and Vogel, 1993), demonstrate that tufa deposition was not restricted to interglacial periods during the last glacial cycle (Tables 2 and 3); albeit, the geomorphological cycle of Ghaap tufa deposition appears to have been inactive during the Last Glacial Maximum. When comparing the radiocarbon and U–Th ages to the stacked benthic $\delta^{18}O$ record of global glacial and interglacial cycles (Lisiecki and Raymo, 2005; Jouzel et al., 2007), it appears that Ghaap tufa growth was more common during interglacial periods than during full glacial conditions (Fig. 3). Variations in local insolation (27°S) are dominated by the precession cycle, but this seems to have little influence on the timing of tufa growth. Sedimentary evidence from the upper part of the Tswaing Crater sedimentary record indicates the increasing importance of regional influences at the expense of the precessional cycle when climatic changes appear to have been driven increasingly by stadial/interstadial cycles after ~50 ka (Partridge, 2002; Holmgren et al., 2003). A radiocarbon age of 44.2 ± 0.8 ka for Groot Kloof tufa GKD_UTH_08 (Table 3) provides evidence of tufa

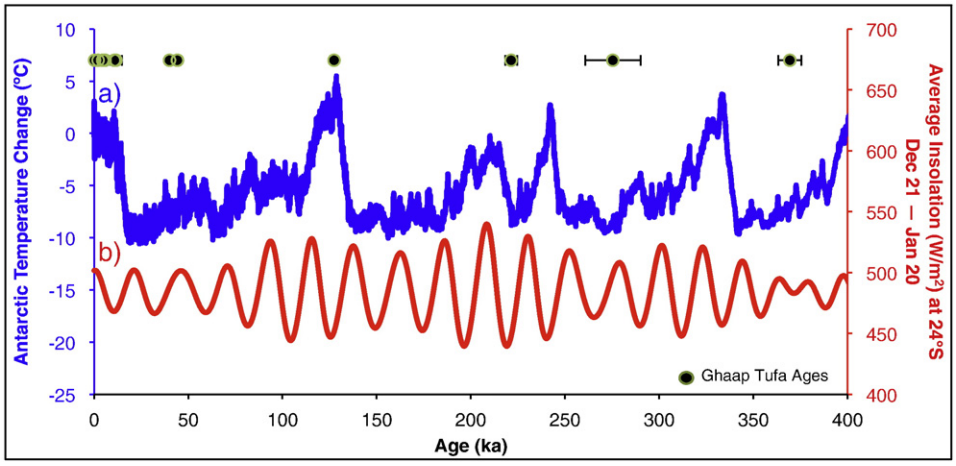

Figure 3. U–Th and ^{14}C ages of Ghaap Plateau escarpment tufas compared with (a) EPICA record of Antarctic temperatures, shown as a heavier line (Jouzel et al., 2007) and (b) December 21st to January 20 mean monthly insolation at 24°S, shown as a lighter line (Laskar et al., 2004) over the last 400 ka illustrating that the Ghaap Plateau escarpment tufa growth was more common during inter-glacial periods than during full glacial conditions.

https://doi.org/10.1016/j.yqres.2015.04.008 Published online by Cambridge University Press

formation matching speleothem growth phases recorded in several southern African caves, including Gladysvale (56–42 ka; Pickering et al., 2007), Lobatse Cave (51 ± 2–43 ± 0.1 ka; Holmgren et al., 1995), and Wolkberg Cave (58 ± 0.6–46 ± 0.3 ka; Holzkämper et al., 2009). The Tswaing Crater sequence indicates humid conditions from ~55 ka to 48 ka followed by a gradual transition from warmer to colder conditions with a short humid period around 40 ka (Scott et al., 2008). Likewise, the carbon isotope record of a stalagmite from Lobatse Cave shows a jump in $\delta^{13}C$ values from −5.5‰ to ~0‰ at ~ 48 ka signalling a transition to drier, colder conditions (Holmgren et al., 1995; Holzkämper et al., 2009). At Wolkberg Cave, the stable isotope record from the upper part of the W5 stalagmite shows a shift towards lower, more variable $\delta^{18}O$ that strongly correlate with the significantly increased carbon isotope values. In conjunction with a change in the primary mineral constitution from calcite to aragonite, the collective evidence from Wolkberg cave indicates a change towards less effective moisture from 58 ka to 46 ka, which is attributed to an increased evaporation/precipitation ratio and progressively drier and colder conditions (Holzkämper et al., 2009). T3 specimen GKD_UTH_08 from this period shows evidence analogous to that of the W5 stalagmite, namely positive carbon isotope values that correlate with a variable oxygen isotope record. It is also notable that this is the only Ghaap tufa specimen analysed with evidence of an aragonite phase, which is interpreted as an indicator of aridity. During glacials, cooler temperatures and reduced evaporation could also lead to increased effective precipitation, even where rainfall was reduced, and thus permit flowstone (Pickering et al., 2007) and tufa formation.

Tufa stable isotopes and paleoenvironments

Petrographic analysis, undertaken to evaluate the influence of diagenetic alteration, demonstrates the preservation of primary fabrics (clotted/peloidal textures, lamination), as well as secondary features (pore-filling cements, micritisation) (Nicoll et al., 1999). Although diagenesis can modify the depositional isotope composition, diagenetic alteration of the Ghaap Plateau escarpment tufa was restricted to cementation of void space, which can occur very early after tufa deposition, generally from waters with the same chemical characteristics, and thereby have no significant effect on the primary isotopic record (Lojen et al., 2004; Arenas-Abad et al., 2010). Moreover, examination of geochemical research on tufas has found no unequivocal evidence that diagenesis is either pervasive or that it significantly changes the depositional stable isotope composition (Andrews, 2006). Based on the collective mineralogical and micromorphological evidence, therefore, the isotopic compositions of the Ghaap Plateau escarpment tufa deposits are considered fairly pristine and reliable records of paleoenvironmental conditions.

Interpretation of paleoenvironmental signals from tufa carbonate geochemistry presents no small challenge, however, owing to the uncertainties introduced by a range of chemical, biological, geomorphic, and hydrologic controls potentially affecting isotopic variability (Andrews, 2006). Despite an imperfect understanding of the formational mechanisms and the short-term environmental variables that can disrupt isotopic equilibrium, the data do allow for broad paleoclimatic interpretations (Andrews et al., 2000). The rapid formation of these deposits typically spanning less than 5000 yr means the geochemical signature reflects paleoenvironmental conditions on a highly resolved temporal scale (Andrews, 2006). At the centimetre scale used in the current study, each sample represents environmental variations averaged out over multi-annual to decadal long periods (Garnett et al., 2004).

The mean oxygen isotope values from the collective Ghaap Plateau escarpment tufa deposits demonstrate a gradual increase from −5.7‰ in the Plio-Pleistocene records, to −3.7‰ in the middle Pleistocene, and to −2.3‰ in the Holocene (Fig. 4a). This trend towards higher $\delta^{18}O$ values with decreasing age parallels that observed in speleothems from the Makapansgat Valley, in northeastern South Africa where late Miocene/early Pliocene mean values of −5.7‰ (Hopley et al., 2007a) increase to −4.9‰ in the Plio-Pleistocene (Hopley et al., 2007b), and to −3.7‰ in the Holocene (Holmgren et al., 2003). Hopley et al. (2007a) and Holmgren et al. (2003) attribute most of this long-term trend to the gradual increase in global ice volume during this time, suggesting that once ice volume changes were taken into account, long-term changes in cave temperature or the isotopic composition of cave dripwaters were small. However, the Pliocene to Holocene ice-volume effect was less than 2‰ and glacial–interglacial variability was less than 1‰ (Shackleton, 1995), indicating that ice volume cannot offer a full explanation for the >4‰ gradual increase in the $\delta^{18}O$ record of the Ghaap Plateau escarpment tufas. The larger increase in $\delta^{18}O$ of the Ghaap tufas indicates that additional processes are contributing to the isotopic trend not present in the speleothem records. To a first approximation, it is expected that both regions of South Africa would have experienced similar (and small) long-term trends in the $\delta^{18}O$ of rainfall and in surface air temperature, and therefore, that these parameters are not responsible for the amplified $\delta^{18}O$ signal in the Ghaap tufa record. Instead, it is more likely that surface water evaporation is the strongest control on the tufa $\delta^{18}O$ trend, as has been demonstrated for tufa deposits from other semi-arid regions (e.g. Smith et al., 2004; Cremaschi et al., 2010).

Modern day mean annual rainfall $\delta^{18}O$ values for South Africa are approximately −3‰ (IAEA/WMO, 2014); at a mean annual temperature of 18°C, modern calcite is precipitated with an $\delta^{18}O$ value of −3.3‰ under conditions of isotopic equilibrium (Craig, 1965). During MIS 3 and 2 (44–24 ka), the $\delta^{18}O$ of Kalahari groundwater averaged −5.6‰ (Kulongoski et al., 2004); assuming a temperature of 15°C equilibrium calcite precipitation would have an $\delta^{18}O$ value of −5.2‰ at this time. Taking global ice volume into account we can make a crude assumption that the $\delta^{18}O$ of rainfall over South Africa was approximately −5.5‰ and −6.5‰ in the Late Pleistocene and Plio-Pleistocene, respectively, and that equilibrium calcite precipitation, likewise, should be approximately −5.5‰ and −6.5‰, assuming a temperature intermediate between glacial and inter–glacial extremes (17°C). Based on these simple calculations, we can infer that the Plio-Pleistocene tufas from the Ghaap plateau are close to their predicted equilibrium $\delta^{18}O$ values of −6.5‰, whereas the middle Pleistocene to Holocene tufas are increasingly isotopically enriched relative to the predicted equilibrium values (Fig. 4a). This is often observed in tufas from a number of other semi-arid regions (e.g. Smith et al., 2004; O'Brien et al., 2006; Cremaschi et al., 2010) as evaporation, degassing, and kinetic effects all tend to increase $\delta^{18}O$ values relative to the predicted equilibrium compositions.

The relatively high carbon isotope values from the Ghaap Plateau escarpment deposits (>−8‰) parallel those observed in tufa from other semi-arid environments where C_4 vegetation is more common (Fig. 4b; Smith et al., 2004). Low $\delta^{13}C$ values can be related to both primary C_3 vegetation and a high soil-derived CO_2 input during periods of low-aridity (Andrews et al., 2000; O'Brien et al., 2006). Within the general trend of tufa carbon and oxygen isotopes, those of the Plio-Pleistocene deposits have the lowest $\delta^{13}C$ values, consistent with well-developed soil profiles and a greater proportion of C_3 vegetation at this time. The lowest $\delta^{13}C$ values from the Plio-Pleistocene tufas deposits (mean: −7.1‰), therefore, likely reflect the input of soil carbon into the DIC of tufa-depositing waters (Chafetz et al., 1991), perhaps indicating only a minor proportion of C_4 vegetation. In contrast, high $\delta^{13}C$ values are commonly associated with either a flora dominated by C_4 plants and/or a deeper introduction of atmospheric CO_2 into the soil during arid stages, when soil respiration is diminished that results in an increase in the ^{13}C of the soil CO_2 (Andrews, 2006). In comparable arid environments, such as Egypt, Kenya, and Arizona, the low negative to low positive $\delta^{13}C$ values of carbonate precipitates have been interpreted as reflecting less soil-zone input due to increased aridity (Smith et al., 2004; O'Brien et al., 2006; Lee et al., 2013). Accordingly,

https://doi.org/10.1016/j.yqres.2015.04.008 Published online by Cambridge University Press

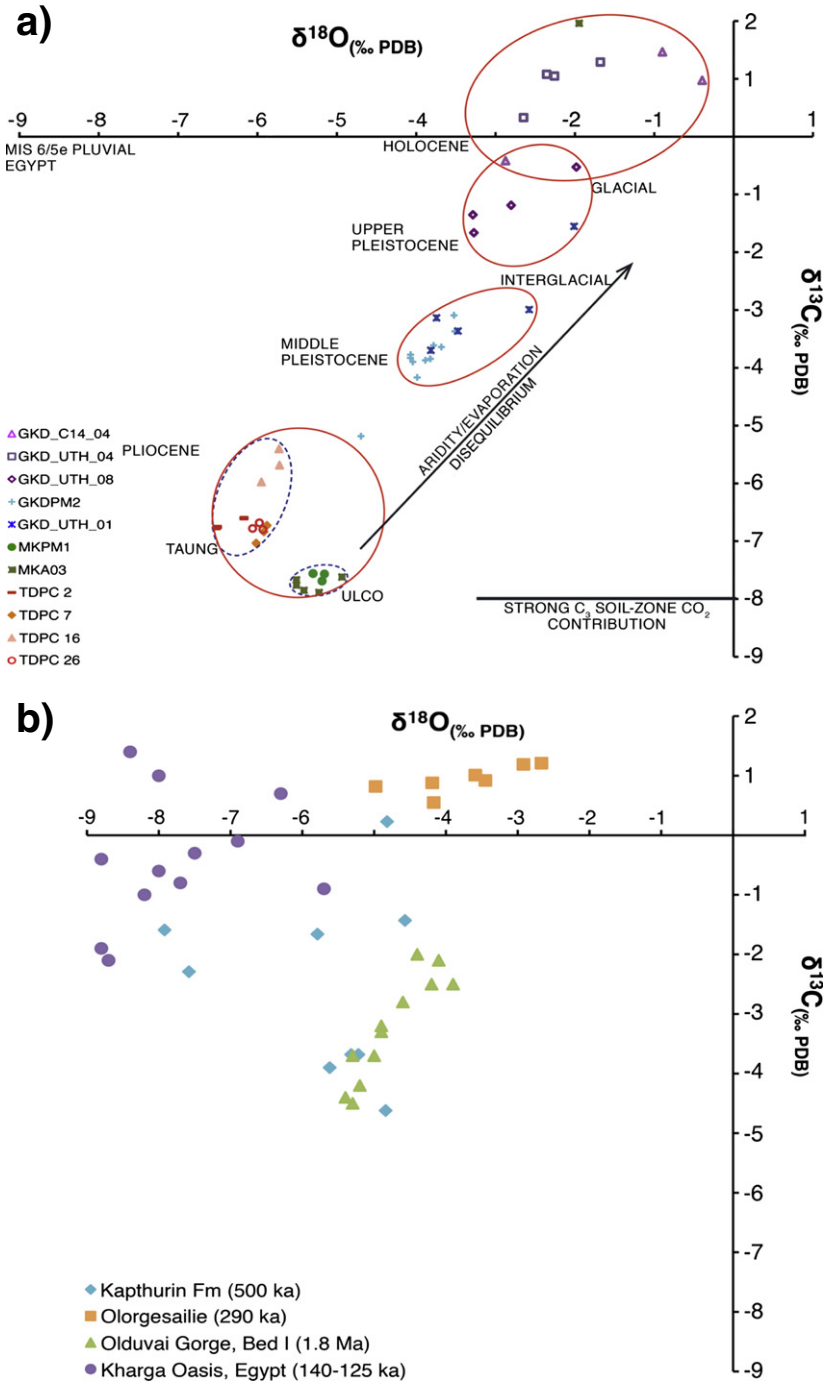

Figure 4. a) Cross-plot of stable isotope data from the Ghaap Plateau escarpment tufa plotted with $\delta^{18}O$ and $\delta^{13}C$ data from Quaternary tufas. The tufa specimens are divided into three distinct groups based on their stable isotope composition reflecting different paleoclimatic regimes: the Plio-Pleistocene Thabaseek Tufa and Malony's Kloof deposits, the Middle Pleistocene Groot Kloof tufa, and the terminal Pleistocene–Holocene deposits from Groot Kloof (including the modern sampling from the tops of MKA_03 and GKD_UTH_01). Collectively, the observed trend in the stable isotope records largely reflects increasing aridity over time in the Ghaap Plateau region of South Africa following the trajectory of increased aridity and evaporation indicated by the marked arrow (after Andrews, 2006). b) Compilation of tufa stable isotope data from east Africa showing overlapping values from the early to late Pleistocene. Data from Kapthurin Formation, Lake Baringo, Kenya (500 ka; Johnson et al., 2009), Olorgesailie, Kenya (290 ka; Lee et al., 2013), Olduvai Gorge, Bed I, FLK NN (1.8 Ma; Ashley et al., 2010), and Kharga Oasis, Egypt (140–125 ka).

the higher $\delta^{13}C$ values obtained for the tufa deposits in the Middle Pleistocene and Holocene groups from the Ghaap plateau (Fig. 4a) are associated with a mixed C_3/C_4 vegetation (as occurs in the modern day), as well as thinner soils in the recharge area (Andrews et al., 1997; Andrews, 2006). Humidity strongly influences the development of flora and soils, which respond to changes in rainfall (Andrews et al., 2000); as such, we would expect to see $\delta^{13}C$ values of tufaecous spring deposits co-vary with the $\delta^{18}O$ evaporation/aridity proxy. Taken together, the observed trend in both tufa $\delta^{18}O$ and $\delta^{13}C$ records is primarily an indicator of increasing aridity over time in the Ghaap Plateau region of South Africa (Fig. 4a). It is interesting to compare this trend with a similar compilation of tufa stable isotope measurements from the early Pleistocene to late Pleistocene of equatorial eastern Africa (see Fig. 4b). The eastern and southern African isotope values are comparable in the late Pleistocene, but they diverge in the Plio-Pleistocene when the South African tufas exhibit lower $\delta^{13}C$ and $\delta^{18}O$ values, suggestive of a less arid environment. In

https://doi.org/10.1016/j.yqres.2015.04.008 Published online by Cambridge University Press

contrast, the East African tufas show a similar degree of aridity in both the early Pleistocene and the late Pleistocene (see Fig. 4b). This may indicate that modern levels of aridity occurred earlier in equatorial east Africa than it did in Southern Africa.

During the Plio-Pleistocene, the combined influence of several large-scale climatic processes directly contributed to the general drying trend characterised by the expansion of C_4 vegetation observed in southern Africa (Maslin and Christensen, 2007). In particular, the Northern Hemisphere Glaciation and corresponding initiation of obliquity paced northern hemisphere glacial cycles, beginning and intensifying between 3.2 and 2.6 Ma, are associated with climatic transitions towards increasingly arid conditions (deMenocal, 2004). These changes manifest terrestrially as an expansion of C_4 grasses predominantly in regions experiencing a reduction in rainfall (Ehleringer et al., 1991, 1997; Hopley et al., 2007a). Analysis of biomineral carbonate $\delta^{13}C$ demonstrates the presence of C_4 vegetation the early Pliocene (Ségalen et al., 2006) with the most significant environmental change to open, grassy landscapes only occurring after 2 Ma when arid conditions became dominant (Hopley et al., 2007a; Lee-Thorp et al., 2007). The Plio-Pleistocene Thabaseek Tufa $\delta^{18}O$ data (−6.5‰ to −5.7‰; mean = −6.0‰; n = 12) correspond well with the $\delta^{18}O$ data of the Miocene/Pliocene Collapsed Cone flowstone (−7.0‰ to −4.5‰; mean = −5.7‰; n = 239) from the Makapansgat Limeworks, South Africa (Hopley et al., 2007a). This indicates that evaporative or kinetic enrichment of $\delta^{18}O$ is not a significant factor in the Thabaseek Tufa, and suggests that a regional $\delta^{18}O$ of rainfall signal is recorded in these tufas. In the Makapansgat Valley speleothem $\delta^{13}C$ records, the Collapsed Cone flowstone exhibits relatively invariant (range of 1.7‰) and more negative (mean = −8.1‰) values when compared with those of the lower part of the Buffalo Cave (1.99 to 1.70 Ma) (mean = −5.7‰) indicative of deposition under two contrasting climatic regimes, before and after the spread of C_4 grasses (Hopley et al., 2007b). The $\delta^{13}C$ record of the Thabaseek Tufa samples ranges from −7.0‰ to −5.4‰ with a mean of −6.5‰, consistent with a predominantly C_3 vegetation, accompanied by the continual but minor presence of C_4 plants. When compared to the Makapansgat record, the higher $\delta^{13}C$ values of the Thabaseek Tufa relative to those from the Collapsed Cone record imply a commensurate increase in the proportion of C_4 grasses; yet not to the degree indicated by the still higher values of the Buffalo cave flowstone. Increases in Thabaseek Tufa $\delta^{13}C$ values reflect periods of increased C_4 vegetation or reduced soil cover occurring in conjunction with increased aridity (as indicated by corresponding higher $\delta^{18}O$ values).

Despite the discontinuous sediment chronology, the isotopic records from the Ghaap Plateau escarpment tufa deposits are consistent with the vegetation and climate trends observed in comparable proxies from southern Africa. Therefore, the complexities of quantifying the $\delta^{18}O$ and $\delta^{13}C$ records in terms of finer-scale processes without additional chronological constraints notwithstanding, the data implicates a strong and repeated climatic control on the geochemical record of the Ghaap Plateau escarpment tufas. The results of the present study highlight the large potential of longer tufa sequences for high-resolution paleoclimate studies in the future.

Conclusion

Since the discovery of the Taung Child, the tufa deposits of the Ghaap Plateau escarpment have been recognized as important geologic records of past hydroclimatic conditions (Butzer, 1974; Butzer et al., 1978). The present study demonstrates the utility of the Ghaap Plateau escarpment tufa deposits to further provide reliable, high-resolution geochemical records of climate change amenable to chronometric dating methods. While this study precluded paleoenvironmental reconstructions, physical and chemical analyses of the Ghaap tufa present clear environmental signals that reflect deposition under distinct paleoclimatic regimes consistent with age. Furthermore, associations with fossil and paleolithic materials encased directly within tufa deposits highlight the value of these sediments not only as climatic archives, but also stratigraphic contexts, as in the case of the *in situ* lithics embedded directly within the Groot Kloof formations. Likewise, deposits at both Groot Kloof and Malony's Kloof may be contemporaneous with Pliocene hominin-bearing deposits at Buxton-Norlim and with which subsequent environmental associations can be made. This initial petrographic and geochemical study of the Ghaap Plateau escarpment tufa deposits has thus demonstrated their reliability as archives of paleoenvironmental information from the Pliocene onwards and, their potential for understanding the paleoclimate of South Africa over the course of hominin evolution.

Acknowledgments

This work was supported by an Australian Research Council (ARC) Future Fellowship grant (FT120100399) and Australian Institute of Nuclear Science and Engineering (AINSE) awards (07/068, 08/031, 08/032) to AIRH. Fieldwork and stable isotope analysis was supported by National Geographic Grants (#8774-10 and #3212) awarded to PJH. We would like to thank Curtis Marean, an anonymous reviewer, and Julian Andrews, who was especially helpful with his time and expertise, for their constructive comments and suggestions on this paper.

Appendix A. Supplementary data

Supplementary data to this article can be found online at http://dx.doi.org/10.1016/j.yqres.2015.04.008.

References

Altermann, W., Wotherspoon, J.M., 1995. The carbonates of the Transvaal and Griqualand West Sequences of the Kaapvaal craton, with special reference to the Lime Acres limestone deposit. Mineral Deposita 30, 124–134.
Andrews, J.E., 2006. Palaeoclimatic records from stable isotopes in riverine tufas: synthesis and review. Earth-Science Reviews 75, 85–104.
Andrews, J.E., Riding, R., Dennis, P.F., 1997. The stable isotope record of environmental and climatic signals in modern terrestrial microbial carbonates from Europe. Palaeogeography, Palaeoclimatology, Palaeoecology 129, 171–189.
Andrews, J.E., Pedley, H.M., Dennis, P.F., 2000. Palaeoenvironmental records in Holocene Spanish tufas: a stable isotope approach in search of reliable climatic archives. Sedimentology 47, 961–978.
Arenas, C., Cabrera, L., Ramos, E., 2007. Sedimentology of tufa facies and continental microbialites from the Palaeogene of Mallorca Island (Spain). Sedimentary Geology 197, 1–27.
Arenas, C., Vázquez-Urbez, M., Auqué, L., Sancho, C., Osácar, C., Pardo, G., 2014. Intrinsic and extrinsic controls of spatial and temporal variations in modern fluvial tufa sedimentation: a thirteen-year record from a semi-arid environment. Sedimentology 61, 90–132.
Arenas-Abad, C., Vázquez-Urbez, M., Pardo-Tirapu, G., Sancho-Mercén, C., 2010. Fluvial and Associated Carbonate Deposits. In: Alonso-Zarza, A. M., Tanner, L. H. (Eds.), Carbonates in Continental Settings: Facies, Environments, and Processes. Developments in Sedimentology. Vol. 61. (Series Ed.: A. J. Van Loon). Amsterdam: Elsevier, pp.133–175.
Ashley, G.M., Dominguez-Rodrigo, M., Bunn, H.T., Mabulla, A.Z.P., Bequedano, E., 2010. Sedimentary geology and human origins: a fresh look at Olduvai Gorge, Tanzania. Journal of Sedimentary Research 80, 703–709.
Beaumont, P.B., Morris, D., 1990. Guide to Archaeological Sites in the Northern Cape. Kimberley, McGregor Museum.
Beaumont, P.B., Vogel, J.C., 1993. What turned the young tufas on at Gorrokop? South African Journal of Science 89, 196–198.
Beaumont, P.B., Vogel, J.C., 2006. On a timescale for the past million years of human history in central South Africa. South African Journal of Science 102, 217–228.
Blackwell, B., Cho, E.K., Herries, A.I.R., Hopley, P., Skinner, A.R., Curnoe, D., 2012. New ESR ages for the Early Stone Age deposits and an early Lechwe (*Kobus leche*) find at Groot Kloof (Northern Cape Province, South Africa). Palaeoanthropology Society Meeting Abstracts, Memphis, TN, 17–18 April 2012, p. A5.
Butzer, K., 1974. Paleoecology of South African australopithecines: Taung revisited. Current Anthropology 15, 367–382.
Butzer, K., Stuckenrath, R., Bruzewicz, A., Helgren, D., 1978. Late Cenozoic paleoclimates of the Gaap Escarpment, Kalahari margin, South Africa. Quaternary Research 10, 310–339.
Carthew, K.D., Taylor, M.P., Drysdale, R.N., 2006. An environmental model of fluvial tufas in the monsoonal tropics, Barkly karst, northern Australia. Geomorphology 73, 78–100.
Chafetz, H.S., Utech, N.M., Fitzmaurice, S.P., 1991. Differences in the δ18O and δ13C signatures of seasonal laminae comprising travertine stromatolites. Journal of Sedimentary Petrology 61, 1015–1028.

Cheng, H., Edwards, R.L., Hoff, J., Gallup, C.D., Richards, C.D., Asmerom, Y., 2000. The half-lives of Uranium-234 and Thorium-230. Chemical Geology 169, 17–33.
Craig, H., 1965. The measurements of oxygen isotope palaeotemperature: stable isotopes in oceanographic studies and paleotemperatures. In: Tongiori, E. (Ed.), Proceedings of the Third Spoleto Conference, Spoleto, Italy. Sischi and Figli, Pisa, pp. 161–182.
Cremaschi, M., Zerboni, A., Spötl, C., Felletti, F., 2010. The calcareous tufa in the Tadrart Acacus Mt. (SW Fezzan, Libya) An early Holocene palaeoclimate archive in the central Sahara. Palaeogeography, Palaeoclimatology, Palaeoecology 287, 81–94.
Curnoe, D., Herries, A., Brink, J., Hopley, P., Van Reyneveld, K., Henderson, Z., Morris, D., 2005. Beyond Taung: palaeoanthropological research at Groot Kloof, Ghaap Escarpment, Northern Cape Province, South Africa. Nyame Akuma 64, 58–65.
Curnoe, D., Herries, A., Brink, J., Hopley, P., Van Reyneveld, K., Henderson, Z., Morris, D., 2006. Discovery of Middle Pleistocene fossil and stone tool-bearing deposits at Groot Kloof, Ghaap escarpment, Northern Cape Province. South African Journal of Science 102, 180–184.
Dart, R.A., 1925. *Australopithecus africanus*: the man-ape of South Africa. Nature 115, 195–199.
deMenocal, P.B., 2004. African climate change and faunal evolution during the Pliocene–Pleistocene. Earth and Planetary Letters 220, 3–24.
Domínguez-Villar, D., Vázquez-Navarro, J.A., Cheng, H., Edwards, R.L., 2011. Freshwater tufa record from Spain supports evidence for the past interglacial being wetter than the Holocene in the Mediterranean region. Global and Planetary Change 77, 129–141.
Ehleringer, J.R., Sage, R.F., Flanagan, L.B., Pearcy, R.W., 1991. Climate change and the evolution of C4 photosynthesis. Trends in Ecology & Evolution 6, 95–99.
Ehleringer, J.R., Cerling, T.E., Helliker, B.R., 1997. C4 photosynthesis, atmospheric CO_2 and climate. Oecologia 112, 285–299.
Ford, T.D., Pedley, H.M., 1996. A review of tufa and travertine deposits of the world. Earth-Science Reviews 41, 117–175.
Garnett, E.R., Andrews, J.E., Preece, R.C., Dennis, P.F., 2004. Climatic change recorded by stable isotopes and trace elements in a British Holocene tufa. Journal of Quaternary Science 19, 251–262.
Hellstrom, J.C., 2003. Rapid and accurate U/Th dating using parallel ion counting multi-collector ICP-MS. Journal of Analytical Atomic Spectrometry 18, 1346–1351.
Hellstrom, J.C., 2006. U–Th dating of speleothems with high initial Th-230 using stratigraphical constraint. Quaternary Geochronology 1, 289–295.
Herries, A., Curnoe, D., Brink, J., Henderson, Z., Morris, D., 2007. Landscape evolution, palaeoclimate and Later Stone Age occupation of the Ghaap Plateau escarpment, Northern Cape Province, South Africa. Antiquity 81, 313.
Herries, A.I.R., Pickering, R., Adams, J.W., Curnoe, D., Warr, G., Latham, A.G., Shaw, J., 2013. A multi-disciplinary perspective on the age of *Australopithecus* in Southern Africa. In: Reed, K.E., Fleagle, J.G., Leakey, R.E. (Eds.), The paleobiology of *Australopithecus*. Springer, Dordrecht, pp. 21–40.
Hogg, A.G., Hua, Q., Blackwell, P.G., Niu, M., Buck, C.E., Guilderson, T.P., Heaton, T.J., Palmer, J.G., Reimer, P.J., Reimer, R.W., Turney, C.S.M., Zimmerman, S.R.H., 2013. ShCal13 Southern Hemisphere Calibration, 0–50,000 years cal bp. Radiocarbon 55, 1889–1903.
Holmgren, K., Karlen, W., Shaw, P.A., 1995. Paleoclimatic significance of the stable isotopic composition and petrology of a Late Pleistocene stalagmite from Botswana. Quaternary Research 43, 320–328.
Holmgren, K., Lee-Thorp, J., Cooper, G., Lundblad, K., Partridge, T., Scott, L., Sithaldeen, R., Talma, A.S., Tyson, P.D., 2003. Persistent millennial-scale climatic variability over the past 25,000 years in Southern Africa. Quaternary Science Reviews 22, 2311–2326.
Holzkämper, S., Holmgren, K., Lee-Thorp, J., Taima, S., Mangini, A., Partridge, T., 2009. Late Pleistocene stalagmite growth in Wolkberg Cave, South Africa. Earth and Planetary Science Letters 282, 212–221.
Hopley, P., Marshall, J., Weedon, G., Latham, A.G., Herries, A.I.R., Kuykendall, K.L., 2007a. Orbital forcing and the spread of C4 grasses in the late Neogene: stable isotope evidence from South African speleothems. Journal of Human Evolution 53, 620–634.
Hopley, P., Weedon, G., Marshall, J., Latham, A.G., Herries, A.I.R., Kuykendall, K.L., 2007b. High- and low-latitude orbital forcing of early hominin habitats in South Africa. Earth and Planetary Science Letters 256, 419–432.
Hopley, P., Herries, A.I.R., Baker, S.E., Kuhn, B., Menter, C., 2013. Brief communication: beyond the South African cave paradigm—*Australopithecus africanus* from Plio–Pleistocene paleosol deposits at Taung. American Journal of Physical Anthropology 151 (2), 316–324.
Horvatinčić, N., Krajcar Bronic, I., Obelic, B., 2003. Differences in the ^{14}C age, ^{13}C and ^{18}O of Holocene tufa and speleothems in the Dinaric karst. Palaeogeography Palaeoclimatology Palaeoecology 193, 139–157.
Humphreys, A.J.B., Thackeray, A.I., 1983. Ghaap and Gariep: Later Stone Age Studies in the Northern Cape. South African Archaeological Society, p. 328.
IAEA/WMO, 2014. Global Network of Isotopes in Precipitation. The GNIP Database. Accessible at. http://iaea.org/water.
Johnson, C.R., Ashley, G.M., De Wet, C.B., Dvoretsky, R., Park, L., Hover, V.C., Owen, R.B., McBrearty, S., 2009. Tufa as a record of perennial fresh water in a semi-arid rift basin, Kapthurin Formation, Kenya. Sedimentology 56, 1115–1137.
Jones, B., Renaut, R. W., 2010. Calcareous Spring Deposits in Continental Settings. In: Alonso-Zarza, A. M., Tanner, L. H. (Eds.), Carbonates in Continental Settings: Facies, Environments, and Processes. Developments in Sedimentology. Vol. 61. (Series Ed.: A. J. Van Loon). Amsterdam, Elsevier, pp. 177–224.
Jouzel, J., Masson-Delmotte, V., et al., 2007. Orbital and millennial antarctic climate variability over the past 800,000 years. Science 317 (5839), 793–796.
Klein, R.G., Cruz-Uribe, K., Beaumont, P.B., 1991. Environmental, ecological, and paleoanthropological implications of the late Pleistocene mammalian fauna from Equus Cave, Northern Cape Province, South Africa. Quaternary Research 36, 94–119.
Kulongoski, J., Hilton, D., Selaolo, E., 2004. Climate variability in the Botswana Kalahari from the late Pleistocene to the present day. Geophysical Research Letters 31, L10204.
Laskar, J., Robutel, P., Joutel, F., Gastineau, M., Correia, A., Levrard, B., 2004. A long-term numerical solution for the insolation quantities of the Earth. Astronomy and Astrophysics 428, 261–285.
Lee, R.K.L., Owen, R.B., Renaut, R.W., Behrensmeyer, A.K., Potts, R., Sharp, W.D., 2013. Facies, geochemistry and diatoms of late Pleistocene Olorgesailie tufas, southern Kenya Rift. Palaeogeography Palaeoclimatology Palaeoecology 374, 197–217.
Lee-Thorp, J.A., Sponheimer, M., Luyt, J., 2007. Tracking changing environments using stable carbon isotopes in fossil tooth enamel: an example from the South African hominin sites. Journal of Human Evolution 53, 595–601.
Lisiecki, L., Raymo, M., 2005. A Pliocene–Pleistocene stack of 57 globally distributed benthic $\delta^{18}O$ records. Paleoceanography 20, 1–17.
Lojen, S., Dolenec, T., Vokal, B., Cukrov, N., Mihelèiæ, G., Papesch, W., 2004. C and O stable isotope variability in recent freshwater carbonates (River Krka, Croatia). Sedimentology 51, 361–375.
Maslin, M.A., Christensen, B., 2007. Tectonics, orbital forcing, global climate change, and human evolution in Africa. Journal of Human Evolution 53, 443–464.
McKee, J.K., 1993a. The faunal age of the Taung hominid fossil deposit. Journal of Human Evolution 25, 363–376.
McKee, J.K., 1993b. Formation and geomorphology of caves in calcareous tufas and implications for the study of Taung fossil deposits. Transactions of the Royal Society of South Africa 48, 307–322.
McKee, J.K., 1994. Catalogue of fossil sites at the Buxton Limeworks, Taung. Palaeontologia Africana 31, 73–81.
Nicoll, K., Giegengack, R., Kleindienst, M., 1999. Petrogenesis of artifact-bearing fossil-spring tufa deposits from Kharga Oasis, Egypt. Geoarchaeology 14, 849–863.
O'Brien, G., Kaufman, D., Sharp, W., Atudorei, V., Parnell, R., Crossey, L., 2006. Oxygen isotope composition of modern and mid-Holocene banded travertine, Grand Canyon, Arizona, USA. Quaternary Research 65, 366–379.
Partridge, T.C., 2000. Hominid-bearing cave and tufa deposits. In: Partridge, T.C., Maud, R.R. (Eds.), The Cenozoic in Southern Africa. Oxford Monographs on Geology and Geophysics 40. Oxford University Press, Oxford, pp. 100–125.
Partridge, T.C., 2002. Were Heinrich events forced from the southern hemisphere? South African Journal of Science 98, 43–46.
Peabody, F.E., 1954. Travertines and cave deposits of the Kaap escarpment of South Africa, and the type locality of *Australopithecus africanus* Dart. Geological Society of America Bulletin 65, 671–706.
Pedley, H.M., 1990. Classification and environmental models of cool freshwater tufas. Sedimentary Geology 68, 143–154.
Pentecost, A., 2005. Travertine. Springer, Berlin.
Pickering, R., Hancox, P., Lee-Thorp, J., Grün, R., 2007. Stratigraphy, U–Th chronology, and paleoenvironments at Gladysvale Cave: insights into the climatic control of South African hominin-bearing cave deposits. Journal of Human Evolution 53, 602–619.
Scott, L., Holmgren, K., Partridge, T.C., 2008. Reconciliation of vegetation and climatic interpretations of pollen profiles and other regional records from the last 60 thousand years in the Savanna Biome of southern Africa. Palaeogeography Palaeoclimatology Palaeoecology 257, 198–206.
Ségalen, L., Renard, M., Lee-Thorp, J.A., Emmanuel, L., Le Callonnec, L., de Rafélis, M., Senut, B., Pickford, M., Melice, J.L., 2006. Neogene climate change and emergence of C4 grasses in the Namib, southwestern Africa, as reflected in ratite 13C and 18O. Earth and Planetary Science Letters 244, 725–734.
Shackleton, N.J., 1995. New data on the evolution of Pliocene climatic variability. In: Vrba, E.S., Denton, G.H., Partridge, T.C., Burckle, L.H. (Eds.), Paleoclimate and evolution, with emphasis on human origins. Yale University Press, New Haven and London, pp. 242–248.
Smith, J., Giegengack, R., Schwarcz, H., 2004. Constraints on Pleistocene pluvial climates through stable-isotope analysis of fossil-spring tufas and associated gastropods, Kharga Oasis, Egypt. Palaeogeography Palaeoclimatology Palaeoecology 206, 157–175.
Vàzquez-Urbez, M., Arenas, M., Pardo, G., 2012. A sedimentary facies model for stepped, fluvial tufa systems in the Iberian Range (Spain): the Quaternary Piedra and Mesa valleys. Sedimentology 59, 502–526.
Viles, H.A., Taylor, M.P., Nicoll, K., Neumann, S., 2007. Facies evidence of hydroclimatic regime shifts in tufa depositional sequences form the arid Naukluft Mountains, Namibia. Sedimentary Geology 195, 39–53.
Vogel, J.C., Partridge, T.C., 1984. Preliminary radiometric ages for the Taung tufas. In: Vogel, J.C. (Ed.), Late Cainozoic Palaeoclimates of the Southern Hemisphere. Balkema, Rotterdam, pp. 507–514.

https://doi.org/10.1016/j.yqres.2015.04.008 Published online by Cambridge University Press